Euclidean Symmetry and the Dynamics of Rotating Spiral Waves

Dwight Barkley
Department of Mathematics and Center for Nonlinear Dynamics, University of Texas, Austin, Texas 78712
and Laboratoire de Physique, Ecole Normale Supérieure de Lyon, 46 Allée d'Italie, 69364 Lyon, France
(Received 1 July 1993)

It is shown that the dynamics of spiral waves in excitable media are organized around a codimension-two point where a Hopf bifurcation from rotating waves interacts with Euclidean symmetry. A simple ordinary-differential-equation model of this bifurcation generates dynamics like the "meandering" of spiral waves.

PACS numbers: 82.20.Mj, 02.20.–a, 82.20.Wt, 87.90.+y

Many nonlinear systems in the laboratory and in nature possess symmetries which markedly influence their dynamics. By incorporating symmetry groups into bifurcation theory, it has been possible to understand precisely how symmetry interacts with dynamics in such nonlinear systems [1]. Despite its successes, symmetric bifurcation theory is not, at present, developed sufficiently to explain the complex, so-called "meandering," dynamics of spiral waves in excitable media [2–14]. The reason, as we shall show, is that the group dictating spiral dynamics is the Euclidean group, E_2, of distance-preserving transformations of the plane (rotations, reflections, and translations), and this noncompact group does not fit into the existing theoretical framework.

In this Letter we present a detailed bifurcation analysis of spiral waves in excitable media. Based on this analysis, we propose a simple low-order system of differential equations to describe spiral dynamics. Specifically, we present a model for the Hopf bifurcation from rotating waves in systems having Euclidean symmetry. The model reproduces the wealth of behavior exhibited by meandering spirals in experiments [3,5,8,9,14] and simulations [4–7,11]. While our starting point and focus is spiral waves in reaction-diffusion systems, the theory presented is entirely general and applicable to all systems of rotating waves in the plane.

We begin by describing the dynamics typical of a single, isolated spiral wave in an excitable medium. Results have been obtained from a detailed numerical study of the reaction-diffusion equations:

$$\frac{\partial u}{\partial t} = \nabla^2 u + \epsilon^{-1} u(1-u)\left[u - \frac{v+b}{a}\right], \quad \frac{\partial v}{\partial t} = u - v, \quad (1)$$

where a, b, and ϵ are parameters with $\epsilon \ll 1$. The v field is taken to be diffusionless, although this is not essential. Equations (1) and numerical methods used to solve them have been described elsewhere [6,10,12,15].

Figure 1 shows a two-parameter phase diagram for the spiral dynamics of Eqs. (1) with $\epsilon = 2 \times 10^{-2}$. Qualitatively similar diagrams are found ubiquitously in surveys of spiral dynamics [4,11,14], and in this sense, Fig. 1 portrays the generic behavior of spiral waves in excitable media. The dynamics in the various regions are illustrated with segments of the path taken by the tip of the spiral as it evolves in time. We use the tip definition in Ref. [6]. For completeness, the region with no spiral solutions to Eqs. (1) is shown, but it will not be considered here.

Rotating waves (RW) are rigidly rotating periodic states that are seen as steady in a frame rotating at the spiral frequency ω_1. Their tip paths form circles. We compute RW solutions by solving a nonlinear eigenvalue problem for the u and v fields, and the frequency ω_1, and then we determine their stability by computing the leading eigenvalues of the associated linear stability operator [12]. The RW states become unstable via a Hopf bifurcation when a complex-conjugate pair of eigenvalues crosses the imaginary axis. This bifurcation introduces a second frequency, ω_2, into the dynamics and gives rise to modulated waves.

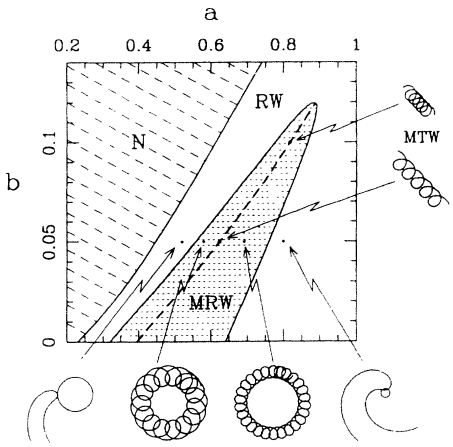

FIG. 1. Phase diagram for spiral-wave dynamics. Shown are regions containing: (N) no spiral waves, (RW) stable rotating waves, and (MRW) modulated rotating waves. Spiral tip paths illustrate states at 6 points. Small portions of spiral waves ($u = 1/2$ contours) are shown for the two RW cases. The MRW tip paths are not closed curves. A locus of supercritical Hopf bifurcations separates the RW and MRW regions. A curve (dashed) of modulated traveling waves (MTW) emerges from the resonant point, $\omega_1 = \omega_2$, on the Hopf locus, and separates MRW states with inward petals (left) and outward petals (right).

0031-9007/93/72(1)/164(4)$06.00

Modulated rotating waves (MRW) are quasiperiodic states that are seen as periodic in a uniformly rotating frame [1,6,16]. In the context of excitable media, these states are referred to as meandering [3] or as compound rotations [9]. We compute MRW states by time-dependent simulations [6,10]. Their tip paths form "flowers" of two distinct types: those with inward petals, which bifurcate with $\omega_2 < \omega_1$, and those with outward petals, which bifurcate with $\omega_2 > \omega_1$. The Hopf locus in Fig. 1 is a smooth curve obtained directly from stability computations. It is everywhere supercritical and flowers grow continuously from circles. (See, e.g., Refs. [5–7,9].)

Emerging from Hopf locus at the point of resonance between the two spiral frequencies, $\omega_1 = \omega_2$, is a locus of modulated traveling waves (MTW). These states are periodic in a uniformly *translating* reference frame [17]. We obtain them by time-dependent simulations in a domain sufficiently large that waves travel significant distances before boundary effects become important. The translation speed increases continuously from zero with distance from the resonant point. (Compare the two MTW states in Fig. 1.) The translation direction is determined by initial conditions. The MTW curve separates the two flower types within the MRW region. Flower sizes (specifically their secondary radii [5,6,9,11]) diverge as the parameter distance from the MTW locus goes to zero, and the MTW states are the limit of either flower type as the flower size diverges.

The resonant Hopf bifurcation is the organizing center for the dynamics in Fig. 1. Arbitrarily close to this codimension-two point there are rotating waves, modulated rotating waves with flowers of both types, and modulated traveling waves. This bifurcation is thus the key to understanding the variety of spiral behavior in Fig. 1.

At linear order, the codimension-two point can be understood from a numerical linear stability analysis of RW solutions. Reference [12] is devoted entirely to this subject. Figure 2(a) shows a RW state at a typical point on the Hopf locus. Its five leading eigenmodes are shown in Figs. 2(b)–2(f) and the corresponding eigenvalue spectrum [18] is illustrated in Fig. 2(g). All other eigenvalues have a negative real part and play no active role in the dynamics. For simplicity, we shall omit reference to the v fields corresponding to Figs. 2(a)–2(f).

Consider first the complex pair of eigenvalues associated with the Hopf bifurcation [squares in Fig. 2(g)]. These eigenvalues are on the imaginary axis only at the Hopf bifurcation; generically they cross the axis transversely as a function of the parameters a and b, and give rise to modulated waves, i.e., the "meandering instability." The associated complex eigenmode is shown in Figs. 2(b) and 2(c), and is discussed in detail in Ref. [12].

The other eigenvalues (crosses) in Fig. 2(g) result from symmetries and are always on the imaginary axis. The eigenvalue at zero is associated with rotational symmetry. The corresponding eigenmode is shown in Fig. 2(d). This mode has been obtained directly from a numerical

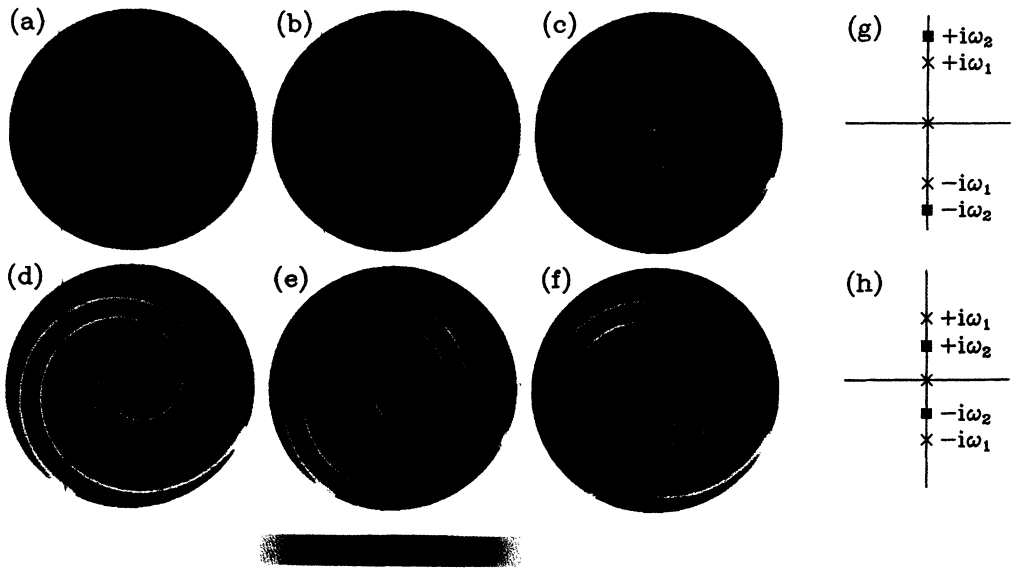

FIG. 2. Linear stability results. (a) Rotating wave (u-field) on the Hopf locus in Fig. 1: $a = 0.760$ and $b = 0.05$. The domain has radius $R = 18$. Blue, black, and red denote $u < 0.1$, $0.1 < u < 0.9$, and $u > 0.9$, respectively. (b)–(f) Leading eigenmodes of (a). The color scale is such that zero values are black and the maximum (minimum) values of each field are white (yellow). (b) and (c) are the real and imaginary parts of the Hopf eigenmode. (d) is the eigenmode resulting from rotational symmetry. (e) and (f) are the real and imaginary parts of the eigenmode associated with translational symmetry. (g) and (h) illustrate eigenvalue spectra on the right and left branches, respectively, of the Hopf locus in Fig. 1. Squares (crosses) denote Hopf (symmetry) eigenvalues.

eigenvalue computation, but its form is precisely that for the rotational mode: $\tilde{u}_R = \partial_\theta u$, where $\tilde{u}_R$ is the eigenmode, u is the RW in Fig. 2(a), and θ is the polar angle.

The complex symmetry eigenvalues in spectrum 2(g), and corresponding complex eigenmode in Figs. 2(e) and 2(f) are associated with translational symmetry. While our finite computational domain is not translationally invariant, we find eigenvalues and eigenmodes which are virtually indistinguishable from those resulting from translational symmetry. It can be verified [12] that in an infinite, homogeneous system, a spiral rotating at frequency ω_1 has translational eigenmodes of the form $\tilde{u}_T = \partial_x u \pm i\partial_y u$, with eigenvalues $\lambda_T = \pm i\omega_1$. Except extremely close to the domain boundary, the eigenmode in Figs. 2(e) and 2(f) is of this form. The associated eigenvalues, λ, are indistinguishable from $\pm i\omega_1$: extrapolation from domains with small radii shows that at radius $R = 18$ (as in Fig. 2), $|\mathrm{Re}(\lambda)| < 10^{-45}$. Hence, these eigenvalues can be considered to lie on the imaginary axis, and therefore the relevant symmetry group for the spiral stability problem is the Euclidean group E_2 of rotations, reflections, *and translations.*

Everywhere on the Hopf locus in Fig. 1, except at the codimension-two point, the five eigenvalues on the imaginary axis are distinct. Apart from the ordering of eigenvalues, there are no qualitative differences between the spectra on the right branch, $\omega_1 < \omega_2$, and those on the left branch, $\omega_1 > \omega_2$, of the Hopf locus [Figs. 2(g) and 2(h)]. At the codimension-two point where $\omega_1 = \omega_2$, the Hopf and translational eigenmodes of the RW state coincide. (Note the similarity between these eigenmodes in Fig. 2.) At this point, the stability operator has eigenvalues $\pm i\omega_1$ each with multiplicity two, plus a zero eigenvalue. This specifies completely the bifurcation to linear order.

We now seek to unfold the resonant Hopf bifurcation, that is to understand in the simplest terms possible the *nonlinear* dynamics which typically exist in the vicinity of such a codimension-two point. However, the bifurcation involves the interaction of Hopf and translational eigenmodes of a rotating wave, and the relevant symmetry group for this problem is E_2. At present, there is no Euclidean-equivariant bifurcation theory from which to obtain a normal form in this case. Therefore, we propose a low-dimensional, weakly nonlinear model which (i) is equivariant under a particular action of E_2, and which (ii) has a Hopf bifurcation from rotating wave solutions. With this model we can gain insight into the codimension-two bifurcation without the complications associated with a partial differential equation system. We leave for the future a rigorous derivation of a low-dimensional model. The model we propose is

$$\begin{aligned} \dot{p} &= v, \\ \dot{v} &= v \cdot \left[f(|v|^2, w^2) + iw \cdot h(|v|^2, w^2) \right], \\ \dot{w} &= w \cdot g(|v|^2, w^2), \end{aligned} \tag{2}$$

where the "position" p and the "velocity" v are complex, and w is real and proportional to frequency. We specify the real-valued functions f, g, and h below. The model is of real dimension five because the codimension-two point has a five-dimensional center eigenspace.

For any choice of f, g, and h, Eqs. (2) are invariant under the following action of E_2:

$$R_\gamma \cdot \begin{pmatrix} p \\ v \\ w \end{pmatrix} = \begin{pmatrix} e^{i\gamma}p \\ e^{i\gamma}v \\ w \end{pmatrix}, \quad \kappa \cdot \begin{pmatrix} p \\ v \\ w \end{pmatrix} = \begin{pmatrix} p^* \\ v^* \\ -w \end{pmatrix},$$

$$T_{\alpha\beta} \cdot \begin{pmatrix} p \\ v \\ w \end{pmatrix} = \begin{pmatrix} p + \alpha + i\beta \\ v \\ w \end{pmatrix},$$

where $*$ denotes complex conjugation. R_γ is rotation by angle γ, κ is reflection, and $T_{\alpha\beta}$ is translation by $\alpha + i\beta$.

Letting $p = x + iy$ and $v = se^{i\phi}$, with "speed" $s \geq 0$, Eqs. (2) become

$$\begin{aligned} \dot{x} = s\cos\phi, \quad \dot{y} = s\sin\phi, \quad \dot{\phi} = w \cdot h(s^2, w^2), \\ \dot{s} = s \cdot f(s^2, w^2), \quad \dot{w} = w \cdot g(s^2, w^2). \end{aligned} \tag{3}$$

We consider the following expansions for f, g, and h:

$$\begin{aligned} f(s^2, w^2) &= \alpha_0 + \alpha_1 s^2 + \alpha_2 w^2 - s^4, \\ g(s^2, w^2) &= -1 + \beta_1 s^2 - w^2, \\ h(s^2, w^2) &= \gamma_0. \end{aligned} \tag{4}$$

Taking into account possible rescalings of v, w, and time, three coefficients have been set to unit magnitude.

The (s, w) subsystem decouples in Eqs. (3), and $\phi(t)$, $x(t)$, and $y(t)$ can be found by quadrature once $s(t)$ and $w(t)$ are known. Rotating waves in the model correspond to nonzero s_1 and w_1 for which $f(s_1^2, w_1^2) = g(s_1^2, w_1^2) = 0$, i.e., steady states in the (s, w) subsystem. It follows that $\phi(t) = \omega_1 t$, where $\omega_1 \equiv \gamma_0 w_1$ and $\phi(0) = 0$. The position, $p = x + iy$, traces out a circle with frequency ω_1.

The bifurcation from rotating to modulated waves in the model is simply a Hopf bifurcation in the (s, w) subsystem. We take α_2 and γ_0 to be bifurcation parameters and fix the other coefficients in (4): $\alpha_0 = -\frac{1}{4}$, $\alpha_1 = \frac{10}{3}$, $\beta_1 = 1$. Then a simple calculation shows that a Hopf bifurcation occurs at $\alpha_2 = -5$ from the rotating wave $(s_1^2, w_1^2) = (\frac{3}{2}, \frac{1}{2})$. The primary frequency is $\omega_1 = \gamma_0 w_1 = \gamma_0/\sqrt{2}$, and the Hopf frequency is $\omega_2 = \sqrt{14}$. Hence a resonance Hopf bifurcation occurs for $\alpha_2 = -5$, $\gamma_0 = \sqrt{28}$. A straightforward calculation shows that at this point the model indeed has the same eigenvalue structure as the codimension-two point in the reaction-diffusion equations.

Figure 3 shows a phase diagram for the model in terms of normalized bifurcation parameters: $\mu \equiv -(\alpha_2 + 5)/5$ and $\nu \equiv \gamma_0/\sqrt{28}$. The Hopf locus is given by $\mu = 0$ with ν determining the frequency ratio at the bifurcation. For $\mu > 0$ there are modulated waves of various types, illustrated with plots of $p(t)$. These bear a striking resemblance to the tip paths of meandering spiral waves in excitable media. See not only Fig. 1, but also plots in Refs. [3–6,8–11,14]. Elsewhere [19], it will be shown that

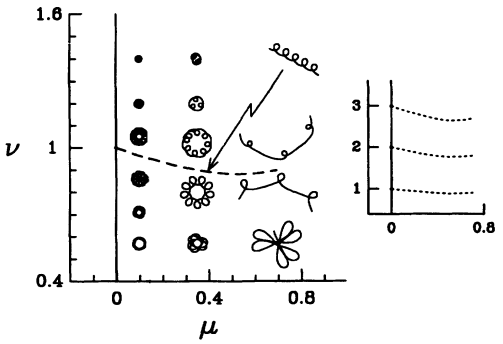

FIG. 3. Phase diagram for the model equations. Numerically obtained plots of $p = x + iy$ over short time intervals are shown centered on corresponding parameter points. The inset shows the three lowest-order resonant bifurcations. Dashed curves show loci of MTW states.

the model reproduces qualitatively all the phenomena in the generic phase diagram for spiral waves, e.g., Fig. 1.

From the model it is possible to extract the scaling laws near resonant bifurcations. We proceed heuristically; a complete treatment gives the same results. Just past the Hopf bifurcation, $s(t)$ and $w(t)$ are of the form (modulo transformations and rescalings):

$$s(t) = s_1 + \sqrt{\mu}\sin(\omega_2 t), \quad w(t) = w_1 + \sqrt{\mu}\cos(\omega_2 t).$$

From these, $\dot{\phi}$ in Eqs. (3) can be integrated to give $\phi(t)$. Substituting this and $s(t)$ into the equations for $\dot{x}$ and $\dot{y}$ in Eqs. (3), one obtains to lowest order in μ

$$\dot{x} \sim s_1\cos(\omega_1 t) + \mu^{1/2}\cos(\omega_1 t)\sin(\omega_2 t) - \frac{\gamma_0 s_1}{\omega_2}\mu^{1/2}\sin(\omega_1 t)\sin(\omega_2 t),$$

and similarly for $\dot{y}$. The dependence of s_1, ω_1, and ω_2 on μ is unimportant here.

The behavior of $p(t) = x(t) + iy(t)$ near a resonant Hopf bifurcation follows immediately. When $\omega_1 = \omega_2$, $\dot{x}$ and $\dot{y}$ have secular terms [e.g., from the product $\sin(\omega_1)\sin(\omega_2)$], and $|p(t)|$ diverges linearly like $\mu^{1/2}t$ as $t \to \infty$. This secular growth is the essence of the MTW dynamics. The translation speed for these MTW states grows from zero as $\mu^{1/2}$. When $\omega_1 \neq \omega_2$, $p(t)$ has terms $(\omega_1^2 - \omega_2^2)^{-1}Q(t)$, where $Q(t)$ is a quasiperiodic function of t. Hence as $(\omega_1 - \omega_2) \to 0$, flower sizes diverge like $(\omega_1 - \omega_2)^{-1}$. It is computationally too costly to determine accurately the scaling exponents for spiral solutions of Eqs. (1); the spiral behavior is nevertheless consistent with the model scalings. In addition to the 1:1 resonance, there are resonant bifurcations in the model at every integer value, k, of ν. See Fig. 3. For a k:1 resonance, it can be shown that the translation speed scales as $\mu^{|k|/2}$. Higher-order, $|k| > 1$, resonances have not been observed for spiral waves.

In conclusion, we have shown that the complex (meandering) dynamics of spiral waves are organized around the codimension-two bifurcation where Hopf eigenmodes interact with eigenmodes resulting from Euclidean symmetry. We have proposed simple model equations for this bifurcation and have shown that these equations generate dynamics strikingly similar to the dynamics of spiral waves. These equations and their bifurcations are of a fundamentally new type from the point of view of symmetric bifurcation theory: as simple as the model equations are, there is no general group-theoretic method which allows one to derive them systematically. Moreover, the dynamics we have examined are not contained, in their entirety, in any normal form based on linear actions of compact groups. It will be of interest to extend symmetric bifurcation theory in the direction suggested by this work.

I thank L. S. Tuckerman and M. Golubitsky for helpful discussions. This work has been supported by NSF Grant No. DMS 92-06224 and NATO Grant No. RCD 92-55315.

[1] M. Golubitsky, I. Stewart, and D.G. Schaeffer, *Singularities and Groups in Bifurcation Theory* (Springer, New York, 1988), Vol. II, and references therein.

[2] References [3–14] are but a select list from the extensive literature on spiral meandering. See Ref. [11] for a more complete list.

[3] A. T. Winfree, Science **181**, 937 (1973).

[4] V. S. Zykov, Biofizika **31**, 862 (1986).

[5] W. Jahnke, W. E. Skaggs, and A. T. Winfree, J. Phys. Chem. **93**, 740 (1989).

[6] D. Barkley, M. Kness, and L. S. Tuckerman, Phys. Rev. A **42**, 2489 (1990).

[7] A. Karma, Phys. Rev. Lett. **65**, 2824 (1990).

[8] T. Plesser, S. C. Müller, and B. Hess, J. Phys. Chem. **94**, 7501 (1990).

[9] G. S. Skinner and H. L. Swinney, Physica (Amsterdam) **48D**, 1 (1991).

[10] D. Barkley, Physica (Amsterdam) **49D**, 61 (1991).

[11] A. T. Winfree, Chaos **1**, 303 (1991).

[12] D. Barkley, Phys. Rev. Lett. **68**, 2090 (1992).

[13] D. A. Kessler, H. Levine, and W. Reynolds, Phys. Rev. A **46**, 5264 (1992).

[14] Z. Nagy-Ungvarai, J. Ungvarai, and S. C. Müller, Chaos **3**, 15 (1993).

[15] M. Kness, L. S. Tuckerman, and D. Barkley, Phys. Rev. A **46**, 5054 (1992).

[16] D. A. Rand, Arch. Rat. Mech. Anal. **79**, 1 (1982).

[17] Normally there is no mathematical distinction between modulated traveling and modulated rotating waves because translational symmetry is treated modulo a spatial period. For spiral waves, however, MRW and MTW states are not equivalent.

[18] As in Ref. [12], we report all stability results as obtained in the frame rotating at the spiral frequency ω_1. These correspond directly to Floquet stability results in the rest frame, e.g., $m = \exp(2\pi\lambda/\omega_1)$, where m is the Floquet multiplier and λ is the eigenvalue in the rotating frame.

[19] D. Barkley and I. G. Kevrekidis (to be published).

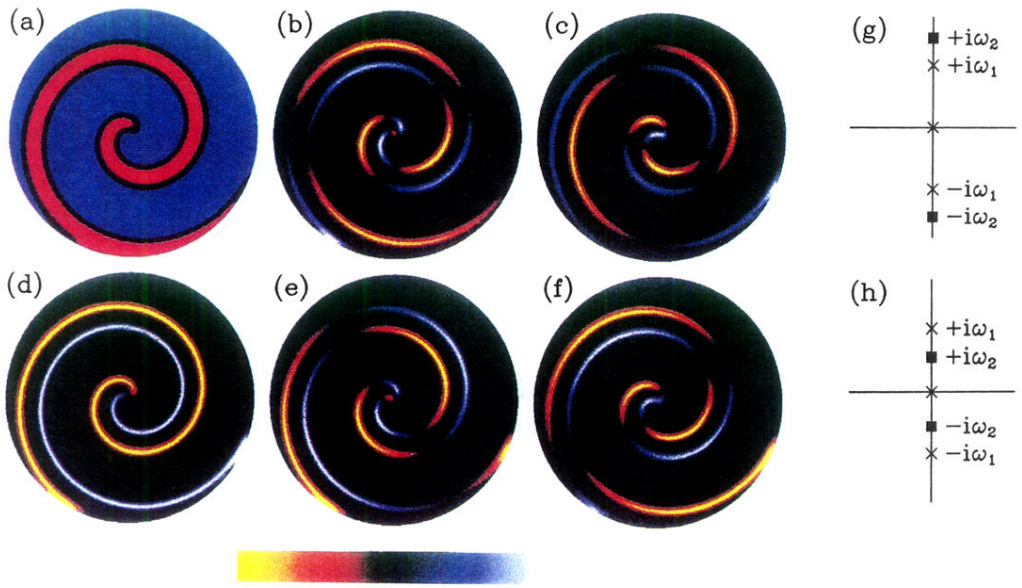

FIG. 2. Linear stability results. (a) Rotating wave (u-field) on the Hopf locus in Fig. 1: $a = 0.760$ and $b = 0.05$. The domain has radius $R = 18$. Blue, black, and red denote $u < 0.1$, $0.1 < u < 0.9$, and $u > 0.9$, respectively. (b)–(f) Leading eigenmodes of (a). The color scale is such that zero values are black and the maximum (minimum) values of each field are white (yellow). (b) and (c) are the real and imaginary parts of the Hopf eigenmode. (d) is the eigenmode resulting from rotational symmetry. (e) and (f) are the real and imaginary parts of the eigenmode associated with translational symmetry. (g) and (h) illustrate eigenvalue spectra on the right and left branches, respectively, of the Hopf locus in Fig. 1. Squares (crosses) denote Hopf (symmetry) eigenvalues.